*Am J Physiol Cell Physiol* 293: C1420–C1425, 2007.
First published August 15, 2007; doi:10.1152/ajpcell.00271.2007.

# A novel method using fluorescence microscopy for real-time assessment of ATP release from individual cells

**Ross Corriden,[2,3,4] Paul A. Insel,[3,4] and Wolfgang G. Junger[1,2,4]**

[1]*Department of Surgery, Beth Israel Deaconess Medical Center and Harvard Medical School, Boston, Massachusetts; and Departments of* [2]*Surgery and* [3]*Pharmacology and Medicine, and* [4]*Biomedical Sciences Graduate Program, University of California, San Diego, California*

Submitted 26 July 2007; accepted in final form 9 August 2007

**Corriden R, Insel PA, Junger WG.** A novel method using fluorescence microscopy for real-time assessment of ATP release from individual cells. *Am J Physiol Cell Physiol* 293: C1420–C1425, 2007. First published August 15, 2007; doi:10.1152/ajpcell.00271.2007.—Many cell types release ATP in response to mechanical or biochemical stimulation. The mechanisms responsible for this release, however, are not well understood and may differ among different cell types. In addition, there are numerous difficulties associated with studying the dynamics of ATP release immediately outside the cell membrane. Here, we report a new method that allows the visualization and quantification of ATP release by fluorescence microscopy. Our method utilizes a two-enzyme system that generates NADPH when ATP is present. NADPH is a fluorescent molecule that can be visualized by fluorescence microscopy using an excitation wavelength of 340 nm and an emission wavelength of 450 nm. The method is capable of detecting ATP concentrations $<1$ μM and has a dynamic range of up to 100 μM. Using this method, we visualized and quantified ATP release from human polymorphonuclear leukocytes and Jurkat T cells. We show that upon cell stimulation, the concentrations of ATP can reach levels of up to 80 μM immediately outside of the cell membrane. This new method should prove useful for the study of the mechanisms of release and functional role of ATP in various cell systems, including individual cells.

purinergic signaling

RELEASE of cellular ATP into the extracellular space is physiologically significant and has been shown to regulate functional responses of excitatory and nonexcitatory cells (4, 6, 12, 23, 30). Released ATP modulates cell function by activating ionotropic P2X and G protein-coupled P2Y receptors (5). Through the activation of these receptors, ATP release is linked to numerous physiological responses, including the "basal" activation of signal transduction pathways and the reaction of cells to mechanical and osmotic stress and membrane deformation during the course of cell migration (7–9, 18, 20, 25, 26, 34).

While the role of ATP as an autocrine and paracrine regulatory signaling molecule has been extensively studied, the precise mechanisms of ATP release from different cells have been difficult to define and likely differ among cell types (3, 10, 11, 15, 30, 32). A major limitation in the study of the mechanisms of ATP release is the lack of methods that allow the visualization of release from individual cells in real time. This shortcoming has made it difficult to determine whether the release of ATP occurs at a specific cellular location and to quantify ATP concentrations in regions close to the cell membrane where they would be highest and where nucleotides would interact with P2 receptors. Incubation of tissues with quinacrine, a fluorescent dye that selectively labels high concentrations of intracellular ATP, was an early and effective, although invasive, method for visualization of granular ATP release from excitatory cells (1, 24). Currently, the most widely used methods to study ATP release are based either on the luciferin/luciferase bioluminescence assay or on HPLC. Both methods allow the quantification of ATP concentrations in bulk media but, as generally employed, cannot provide direct information regarding concentrations in membrane microenvironments that are relevant for the cellular responses to ATP. Several elegant methods have been proposed to overcome this limitation, including the use of ATP biosensors (2, 13, 14, 19, 21, 27) and measurements of the changes in fluorescent properties of luciferin after its conversion by luciferase (31). While powerful, these techniques are sometimes technically challenging, often requiring generation and/or positioning of reporters in a manner that does not allow for visualization of rapid dynamics of ATP release from individual cells.

Here, we present a method that utilizes fluorescence microscopy to visualize ATP release from individual cells and to estimate the concentrations of ATP at different regions in the extracellular space. The assay is based on a tandem enzyme reaction driven by hexokinase and glucose-6-phosphate dehydrogenase (G6PD), which, in the presence of ATP and glucose, converts NADP to NADPH at an equimolar ratio. NADPH is a highly fluorescent compound that can be easily imaged using fluorescence microscopy (28). This conceptually simple assay has the potential to be easily adapted for use by laboratories interested in the study of a wide variety of cellular systems in which ATP release and responses may be involved.

## MATERIALS AND METHODS

*Materials.* Unless otherwise indicated, all chemicals were obtained from Sigma-Aldrich Chemical (St. Louis, MO). HBSS was from Irvine Scientific (Santa Anna, CA). Phytohemagglutinin was from Roche Applied Science (Indianapolis, IN).

*Microscope system.* All microscope experiments were performed using an inverted Leica DMIRB microscope (Leica, Wetzlar, Germany) equipped with a PSMI-2 stage incubator controlled by a TC-202A temperature controller (Harvard Apparatus, Holliston, MA) and a Hamamatsu Orca II camera (Hamamatsu, Hamamatsu City, Japan). Images were acquired using Openlab software (Improvision, Coventry, UK). Based on the fluorescence properties of NADPH, we used a filter set consisting of a 340-nm band-pass exciter with a band

Address for reprint requests and other correspondence: W. G. Junger, Dept. of Surgery, Beth Israel Deaconess Medical Center and Harvard Medical School, Boston, MA 02215 (e-mail: wjunger@bidmc.harvard.edu).

The costs of publication of this article were defrayed in part by the payment of page charges. The article must therefore be hereby marked "*advertisement*" in accordance with 18 U.S.C. Section 1734 solely to indicate this fact.


0363-6143/07 $8.00 Copyright © 2007 the American Physiological Society


Downloaded from http://ajpcell.physiology.org/ by 10.220.33.3 on September 23, 2017

width of 30 nm (Omega Optical, Brattleboro, VT), a 450-nm band-pass emitter with a band width of 40 nm (Chroma Technology, Rockingham, VT), and a 400-nm dichroic mirror (Chroma Technology). UV illumination was generated using a 100-W short-arc mercury lamp (Ushio, Tokyo, Japan). The microscope was isolated from vibrations using a TMC Micro-g63-542 vibration isolation table (Technical Manufacturing, Peabody, MA). To generate an ATP gradient and to mechanically perturb cells, we used an InjectMan NI 2 micromanipulator in combination with a FemtoJet microinjection system from Eppendorf (Hamburg, Germany).

*Cell culture and polymorphonuclear neutrophil isolation.* The human Jurkat T cell line (American Type Culture Collection, Manassas, VA) was cultured in RPMI supplemented with 10% heat-inactivated FCS (Omega Scientific, Tarzana, CA). Human polymorphonuclear neutrophils (PMNs) were isolated from peripheral blood of healthy adult volunteers as previously described (16). This study was approved by the Institutional Review Board of the University of California-San Diego.

*Optical properties of NADPH.* As shown in Fig. 1*A*, increasing concentrations of ATP elicit the conversion of corresponding concentrations of NADP to NADPH. NADPH has a maximum absorbance at 340 nm (28). An emission spectrum generated using a SFM25 Kontron spectrofluorometer (Kontron Instruments, Basel, Switzerland) set to an excitation wavelength of 340 nm showed a maximum emission peak at a wavelength of 450 nm (Fig. 1*B*). Based on these data, we chose a filter set for our microscope system consisting of a 340 ± 15-nm bandpass exciter, a 450 ± 20-nm band-pass emitter, and a 400-nm dichroic mirror to detect the fluorescent signal of NADPH.

*Detection of exogenous ATP.* All experiments were performed using an assay solution containing 2 U/ml hexokinase (catalog no. H-6380, Sigma), 2 U/ml G6PD (catalog no. G-5885, Sigma), 2 mM NADP (catalog no. N-1511, Sigma), and 10 mM D-glucose (catalog no. G-400, Sigma) diluted in HBSS. Depending on the experimental design, ATP was either added to this solution in bulk or was slowly released into the solution at constant rate from a micropipette tip. We used a Leica PL Fluotar oil-immersion objective with a magnification of ×100 and a nominal aperture of 1.30 and recorded images with the Orca II camera using a 700-ms exposure time. Openlab software was used to extract fluorescence intensity values (expressed as gray values) from recorded images. Gray values from selected regions of interest (ROIs) were averaged and converted to ATP concentrations using standard curves generated with ATP standard solutions.

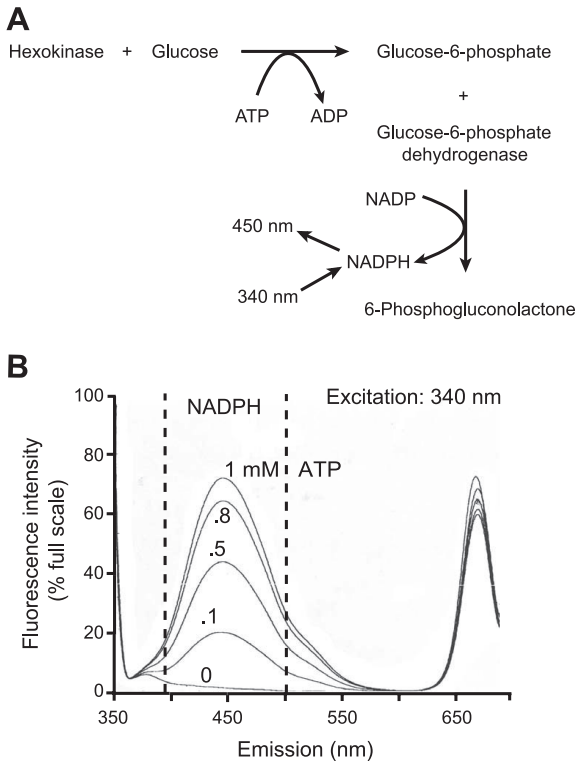


Fig. 1. Assay system used to visualize ATP release. *A*: summary of the tandem enzyme reaction resulting in the formation of the fluorescent product NADPH in the presence of ATP and glucose. *B*: emission spectra of assay mixtures after the addition of increasing concentrations of ATP. Emission data were obtained with a SFM25 Kontron spectrofluorometer adjusted to an excitation wavelength of 340 nm. The emission peak at 450 nm corresponds to NADPH.

*Detection of ATP using the luciferase assay.* A luciferase/luciferin method standard curve was generated using the Roche Applied Science ATP Bioluminescence Assay Kit (Roche Diagnostics). Equal volumes (100 μl) of ATP solution and the luciferase/luciferin substrate mixture provided with the kit were placed in a Turner Designs 20/20 luminometer (Turner Designs; Sunnyvale, CA), and the luminescence was measured by integration over a 3-s time interval. These measurements were repeated three times and expressed as an average.

*Stimulation of ATP release from cells.* To remove existing extracellular ATP, Jurkat cells or PMNs were gently washed three times with fresh HBSS and allowed to settle at room temperature. Cells were then gently resuspended in 50 μl HBSS supplemented with 10 mM D-glucose and placed onto a coverslip in a stage incubator with the temperature set to 37°C. To minimize the release of ATP due to mechanical stress, cells were kept on a vibration isolation table for the entire duration of the experiment. Before ATP release was assayed, 50 μl of a 2× concentrated assay solution containing enzymes and substrate were added to the cells. For experiments where ATP was released through cell lysis or osmotic stress, 10 μl of a 1% Triton X-100 solution in HBSS or 10 μl of 1,000 mM NaCl solution in HBSS, respectively, were added to cells. For experiments with activated Jurkat cells, 1 μl of a suspension of $1 \times 10^7$ Macsibeads/ml coated with anti-CD3 and anti-CD28 antibodies as specified for the Macsibeads kit (Miltenyi Biotech, Bergisch Gladbach, Germany) was incubated with cells. In experiments using PMNs, cells were stimulated with a solution of 100 nM formyl-methionyl-leucyl-phenylalanine peptide (fMLP; Sigma), which was released from a micropipette tip. To account for cellular autofluorescence in ROIs above the cell body, initial gray value readings in these regions were obtained and then subtracted from subsequent readings obtained after cell stimulation. For each type of stimulation, control experiments were performed without NADP in the substrate mixture to ascertain that cell stimulation did not alter autofluorescence readings.

## RESULTS AND DISCUSSION

*Optimizing the fluorescence ATP assay system.* The hexokinase/G6PD reaction has previously been used to quantify glucose concentrations (22). The two-step reaction, as shown in Fig. 1*A*, hydrolyzes ATP, resulting in the formation of equimolar concentrations of NADPH, a strongly fluorescent product with an absorption maximum at 340 nm (28). We evaluated the emission spectrum using a SFM25 Kontron spectrofluorometer (Kontron Instruments) set to an excitation wavelength of 340 nm (Fig. 1*B*). Based on these data, we chose an appropriate filter set (as described in MATERIALS AND METHODS) for the microscope setup used in our application.

We then tested various enzyme and substrate concentrations in a cell-free system to determine those that would be optimal for our assay so as to maximize the speed of the sequential reactions that lead to the formation of NADPH. This is particularly important in cell systems where the half-life of extracellular ATP is reduced by ectoenzymes that hydrolyze the nucleotide (36). To maximize reaction speed, we optimized the



Downloaded from http://ajpcell.physiology.org/ by 10.220.33.3 on September 23, 2017

concentrations of the enzymes (hexokinase and G6PD) and of the substrates (NADP and glucose). The effect of the substrate/enzyme concentrations on the rate of NADPH generation was tested by adding increasing concentrations of the reaction components to HBSS and monitoring the speed of NADPH formation in response to the addition of 1 mM ATP using fluorescence microscopy. To avoid substrate limitation, the concentration of NADP in the assay solution had to exceed maximum concentrations of ATP expected in the extracellular space, which was estimated to be ~50 μM (13). We found that 2 mM NADP yielded optimal results and the highest reaction speed. However, NADP concentrations of >2 mM reduced the reaction speed, possibly due to substrate inhibition (Fig. 2*A*), as previously described for some isoforms of G6PD (33). Increasing the concentrations of hexokinase (Fig. 2*B*) or G6PD (Fig. 2*C*) increased the conversion of 2 mM NADP to NADPH. Based on these experiments, we determined that 2 U/ml of each enzyme was optimal to maximize reaction speed. Higher enzyme concentrations did not significantly increase reaction velocity.

As shown in Fig. 1, the tandem reaction requires glucose as a cosubstrate. We tested if increasing the glucose concentration would increase the reaction speed in our assay system. Predictably, the addition of 10 or 20 mM glucose to the 5.5 mM glucose contained in HBSS increased the initial rate of the reaction from 10 to 60 fluorescence units/s (gray value); however, only minimal increases in the reaction rate were seen when >10 mM glucose was added (Fig. 2*D*). This may be a result of substrate inhibition (29). Based on the data from experiments shown in Fig. 2, we determined that the following assay mixture resulted in a maximal reaction speed: 2 U/ml hexokinase, 2 U/ml G6PD, 2 mM NADP, and 10 mM D-glucose. All components were diluted in HBSS.

Using these assay components in the microscope setup described above, we found that an exposure time of 700 ms was necessary to capture fluorescent signals of low concentrations of NADPH. Increasing the exposure time of the camera to 1,000 ms did not significantly improve the resolution of the assay because of increased background noise. Therefore, we set the camera exposure time to 700 ms for all experiments.

*Verification of the fluorescence microscope assay system.* To test the ability of the assay system described above to detect ATP concentration gradients, we used a solution of 100 μM ATP in HBSS in a micropipette mounted on a microinjector system and slowly released ATP into a solution containing the enzyme and substrate mixture. We obtained a fluorescence signal that emanated from the micropipette tip and increased in intensity as a function of time as a consequence of ATP accumulation around the pipette tip (Fig. 3*A*). Repeating this experiment using lower concentrations of ATP revealed a similarly rapid conversion of NADP to NADPH at the site of ATP release, although lower fluorescence intensities were observed (data not shown).

We used ATP standard solutions to estimate ATP concentrations using this assay. Solutions of increasing ATP concentrations were added to the assay solution, and reactions were allowed to go to completion. Samples of each solution were placed on coverslips, and, using the microscope settings described above, fluorescence images were obtained to determine the NADPH fluorescence signal corresponding to each ATP concentration. Because the concentration of ATP, and therefore NADPH, was uniform for each sample, we were able to extract the average gray value from each image and correlate these values to respective ATP concentrations. These signals increased in a nearly linear fashion at ATP concentrations between 0 and 400 μM (Fig. 3*B*). At higher ATP concentrations, the fluorescence signal reached a plateau.

We compared the sensitivity and range of our method with those of the luciferin/luciferase assay that is commonly used to measure ATP concentrations in bulk solutions. The luciferin/luciferase assay was more sensitive and had a broader dynamic range extending from the low nanomolar to millimolar range (Fig. 3*C*). Several groups (2, 30) have previously noted that extracellular ATP can reach concentrations as high as 100 μM. Thus, our method can detect the dynamics of release of such ATP concentrations, despite its more limited dynamic range and sensitivity compared with luciferin/luciferase.

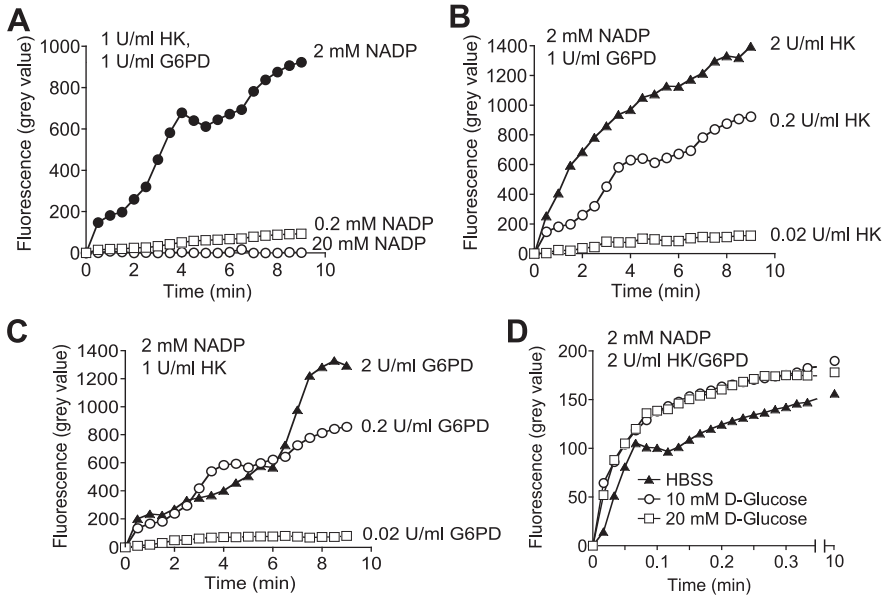


Fig. 2. Optimization of the ATP assay. *A*: effect of increasing concentrations of the substrate NADP on kinetics of the tandem enzyme assay in a cell-free system. Increasing concentrations of NADP were added to HBSS containing 1 U/ml hexokinase (HK), 1 U/ml glucose-6-phosphate dehydrogenase (G6PD), and 1 mM ATP, and fluorescence intensity (gray values) was measured over 10 min. *B*: increasing concentrations of HK were added to HBSS containing 2 mM NADP, 1 U/ml G6PD, and 1 mM ATP. Changes in fluorescence intensity were measured over a period of 10 min. *C*: increasing concentrations of G6PD were added to HBSS containing 2 mM NADP, 1 U/ml HK, and 1 mM ATP, and fluorescence intensity was measured over 10 min. *D*: increasing concentrations of D-glucose were added to HBSS containing 2 U/ml HK, 2 U/ml G6PD, 2 mM NADP, and 100 μM ATP. Changes in fluorescence intensity were measured over 10 min.



Downloaded from http://ajpcell.physiology.org/ by 10.220.33.3 on September 23, 2017

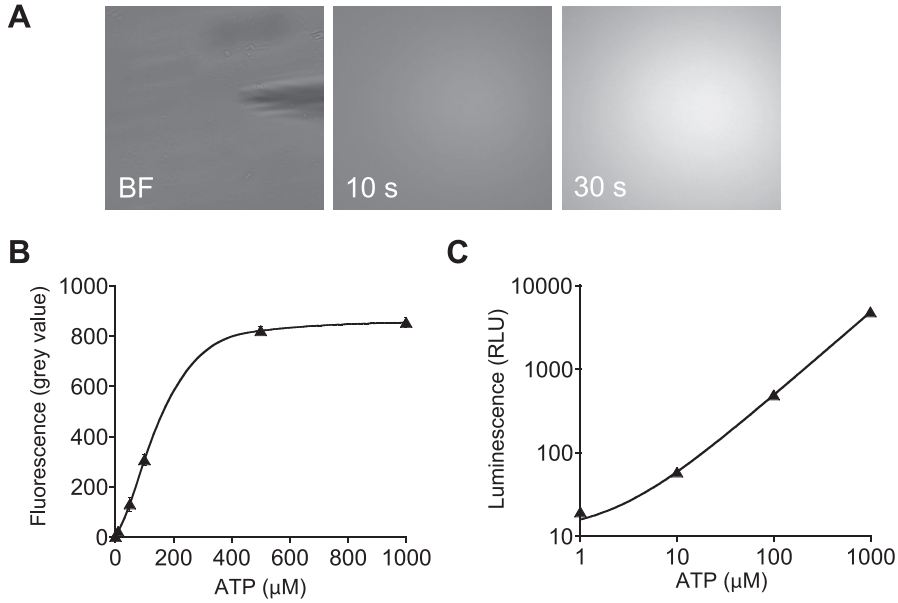


Fig. 3. Quantification of the ATP assay. *A*: ATP (100 μM) was released from a pipette tip into an assay mixture consisting of 2 U/ml HK, 2 U/ml G6PD, and 2 mM NADP in HBSS with 4.5 mM additional glucose, and NADPH formation was visualized using fluorescence microscopy. BF, baseline fluorescence. *B*: ATP response of the fluorescence assay. Increasing concentrations of ATP were added to the assay mixture described above, and fluorescence intensity (gray values) were recorded by fluorescence microscopy, averaged, and plotted against ATP concentration. *C*: ATP response of the luciferin/luciferase luminescence assay. Increasing concentrations of ATP were added to the assay described above, and relative luminescence units (RLUs) were determined as described in MATERIALS AND METHODS.

*Visualization of ATP release from living cells.* After establishing that our fluorescence assay system was potentially suitable to visualize and quantify physiologically relevant ATP concentrations, we tested directly if this system would allow the visualization and quantification of ATP release from living cells. As a first step for validating our method, we sought to visualize ATP release during lysis of Jurkat T cells. Cells were placed onto an inverted microscope, bathed in the assay mixture, and lysed with Triton X-100 to release their cytosolic ATP (Fig. 4, *A* and *B*). Cell lysis rapidly increased NADPH fluorescence, corresponding to 10 μM ATP (Fig. 4*B*). This fluorescence signal rapidly dissipated, probably as a consequence of dilution or hydrolysis of ATP by ectonucleotidases and related enzymes. In the absence of hexokinase, we observed no increase in the fluorescence signal. However, we noted autofluorescence of untreated cells in the experiments

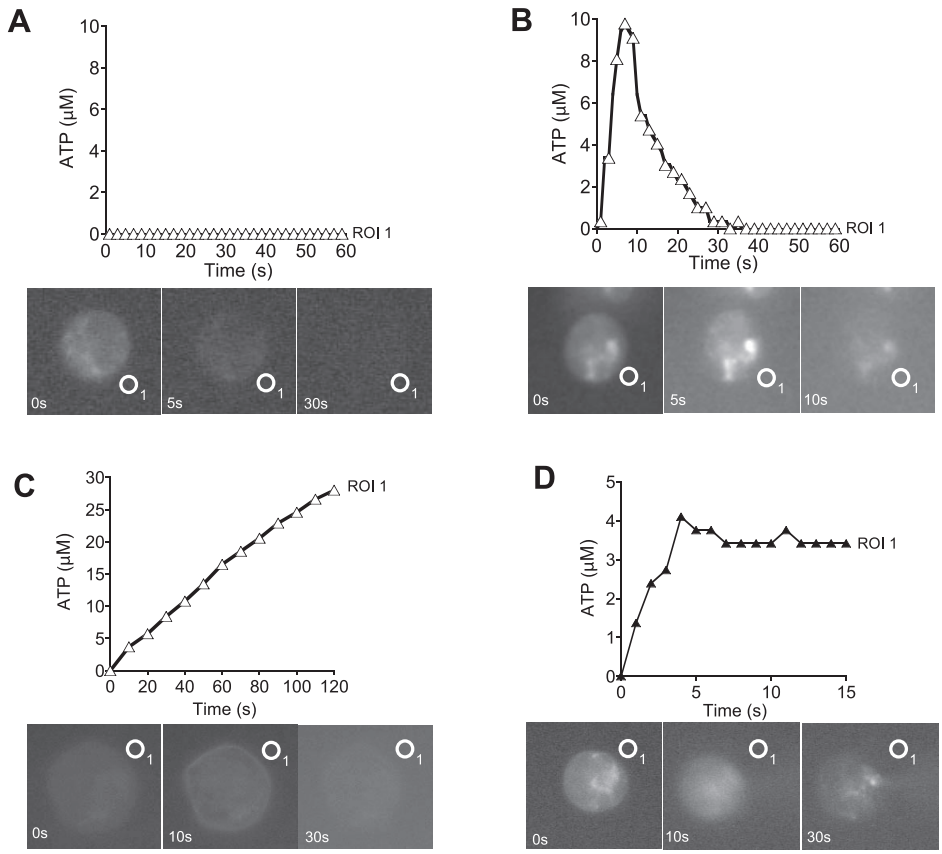


Fig. 4. Application of the NADPH-based fluorescence microscope assay to visualize ATP release from living cells. Frames at the *bottom* of *A–D* show image sequences with regions of interest (ROIs) marked with numbered circles (*ROI 1*), at which average fluorescence intensities (gray values) were determined. Graphs at the top of *A–D* depict the corresponding ATP concentrations determined with ATP standard curves as shown in Fig. 3*B*. *A*: Jurkat T cell lysed with 0.1% Triton X-100 in the absence of assay solution. *B*: Jurkat T cell lysed with 0.1% Triton X-100 in the presence of assay solution. *C*: Jurkat T cell treated with 20 mM hypertonic solution (HS). *D*: release of ATP from a Jurkat T cell after mechanical stimulation with a micropipette tip.



Downloaded from http://ajpcell.physiology.org/ by 10.220.33.3 on September 23, 2017

shown in both Fig. 4, *A* and *B*, suggesting that our optical assay system can detect the fluorescence signal generated by endogenous NADH or NADPH within cells. Upon cell lysis, this autofluorescence signal rapidly disappeared and became undetectable after 30 s (Fig. 4*A*).

Hyperosmotic conditions can rapidly release ATP from Jurkat T cells (20). We tested if we could visualize this ATP release with our assay system. We added a small aliquot of 1 M NaCl to Jurkat T cells bathed in assay solution to increase the osmolarity of the culture medium by 20 mM. After the addition of NaCl, ATP was rapidly (<10 s) released (Fig. 4*C*). Quantification of the signal in a ROI outside of the cell revealed a steady release of ATP, increasing extracellular ATP concentration by 15 μM within 60 s after exposure of the Jurkat cells to hyperosmotic conditions (Fig. 4*C*).

A primary goal for developing the fluorescence assay described here was to allow the visualization of ATP release during cellular activation. To this end, we assessed ATP release in response to stimulation of two different cell types: Jurkat T cells and human PMNs. Jurkat T cells were stimulated with beads coated with antibodies to CD3 and CD28, which stimulate the receptors required for T cell activation. PMNs were stimulated with the bacterial cell wall-derived chemoattractant formyl peptide (fMLP). Both treatments have been previously shown to induce robust ATP release (7, 8, 20, 35). Immediately after stimulation of Jurkat T cells, we found that ATP was released from the entire area of the cell membrane and liberally emanated from the cells some distance into the extracellular space (Fig. 5*A*, compare signal at *ROI 1* vs. *ROI 2*). The NADPH signal was particularly strong at localized membrane regions, suggesting the existence of distinct and spatially segregated ATP release sites. A region selected immediately outside the cell membrane (*ROI 1*) revealed that ATP concentrations in the extracellular space close to the cell membrane reached ~80 μM within 2 min of initiation of cell stimulation. Figure 5*B* shows the response of Jurkat T cells to stimulation with a second type of stimulus, the lectin phytohemagglutinin (10 μg/ml). ATP release occurred at a nearly constant rate with ATP emanating far into the extracellular space, where ATP concentrations of ~20 μM were observed within 2 min of cell stimulation.

In contrast to T cells, stimulation of PMNs with 10 nM fMLP caused polarization of cells and concomitant polarized ATP release. In the experiment shown in Fig. 5*C*, we estimated the concentrations of ATP in three separate ROIs. *ROI 1* was chosen within the cell body at an area with dynamic changes in ATP concentrations. *ROI 2* was selected at another site within the cell body, and *ROI 3* was chosen close to the uropod (i.e., the trailing edge) of the same cell. At these different sites, we observed different dynamics of ATP release with concentrations of ATP increasing to 25 μM, a value that is consistent with data reported previously by others (14). The release of ATP at the cell surface (*ROI 1*) seemed to occur in fluctuating bursts, suggesting that release occurs via degranulation. In contrast, ATP release at *ROI 2* showed less fluctuation. ATP close to the uropod (*ROI 3*) remained low and did not fluctuate, implying that fMLP stimulation did not promote the release of ATP from that region of the cell. Assessment of the concentration of ATP at the leading edge of PMNs in the process of cell migration, as shown in Fig. 5*D*, revealed that ATP concentrations at the leading edge (*ROI 1*) increased concomitantly with pseudopod protrusion, whereas little ATP was

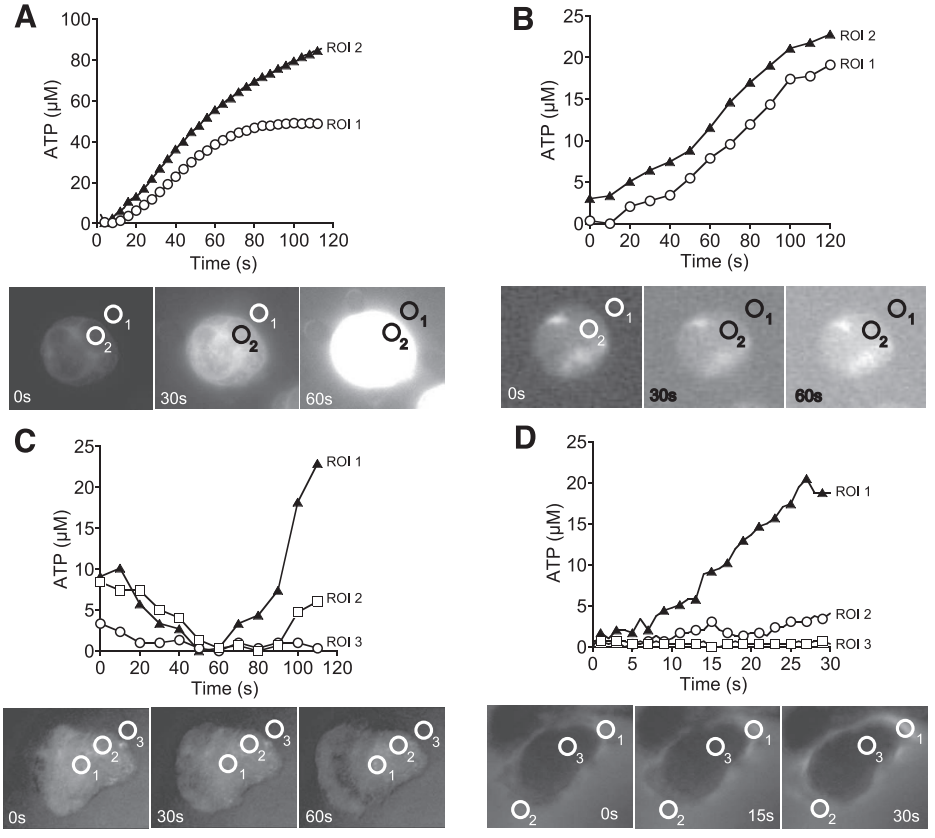


Fig. 5. Detection of ATP release of different immune cell types in response to physiological cell stimulation. *A*: Jurkat T cell stimulated with anti-CD3/CD28 antibodies bound to microbeads. *B*: Jurkat T cell stimulated with phytohemagglutinin. *C*: human peripheral blood neutrophil stimulated with 10 nM formyl-methionyl-leucyl-phenylalanine peptide (fMLP). *D*: release of ATP from a migrating human neutrophil stimulated with 10 nM fMLP. Numbers with circles indicate *ROI 1–ROI 3*, areas from which average fluorescence intensities (gray values) were determined.



Downloaded from http://ajpcell.physiology.org/ by 10.220.33.3 on September 23, 2017

released at the uropod (*ROI 2*) or in the center of the cell body (*ROI 3*).

ATP release from cells occurs in a three-dimensional space. The determination of ATP concentrations in a three-dimensional space would require confocal microscopy. The two-dimensional microscopy method shown here suffers from the limitation that it cannot resolve ATP concentration differences along the *z*-plane. These problems could be overcome with more sophisticated equipment such as spinning disc confocal or two-photon microscopy systems.

In conclusion, the assay system described here allows the detection of ATP release from living cells. Using this assay, we show that Jurkat T cells and isolated human PMNs differ profoundly with regard to the concentration and speed of ATP that they release as well as in the subcellular locales from which ATP release occurs. This new assay should prove useful for the visualization and quantification of ATP release, including from single cells, and may provide a convenient means to study spatiotemporal aspects of ATP release from numerous cell types and tissue preparations.

## GRANTS

This work was supported in part by National Institutes of Health (NIH) Grants R01 GM-51477 and GM-60475 (to W. G. Junger) and GM 66232 (P. A. Insel); by Congressionally Directed Medical Research Program Grant PR043034 (to W. G. Junger); and by NIH Predoctoral Training Grant DK-07202 (to R. Corriden).

## REFERENCES

1. **Alund M, Olson L.** Depolarization-induced decreases in fluroescence intensity of gastro-intestinal quinacrine-binding nerves. *Brain Res* 166: 121–137, 1979.
2. **Beigi R, Kobatake E, Aizawa M, Dubyak GR.** Detection of local ATP release from activated platelets using cell surface-attached firefly luciferase. *Am J Physiol Cell Physiol* 276: C267–C278, 1999.
3. **Bell PD, Lapointe JY, Sabirov R, Hayashi S, Peti-Peterdi J, Manabe K, Kovacs G, Okada Y.** Macula densa cell signaling involves ATP release through a maxi anion channel. *Proc Natl Acad Sci USA* 100: 4322–4327, 2003.
4. **Bodin P, Burnstock G.** Purinergic signalling: ATP release. *Neurochem Res* 26: 959–969, 2001.
5. **Burnstock G.** Purinergic signalling. *Br J Pharmacol* 147, *Suppl* 1: S172–S181, 2006.
6. **Burnstock G.** Physiology and pathophysiology of purinergic neurotransmission. *Physiol Rev* 87: 659–797, 2007.
7. **Chen Y, Corriden R, Inoue I, Yip L, Hashiguchi N, Zinkernagel A, Nizet V, Insel PA, Junger W.** ATP release guides neutrophil chemotaxis via P2Y2 and A3 receptors. *Science* 314: 1792–1795, 2006.
8. **Chen Y, Shukla A, Namiki S, Insel PA, Junger WG.** A putative osmoreceptor system that controls neutrophil function through the release of ATP, its conversion to adenosine, and activation of A2 adenosine and P2 receptors. *J Leukoc Biol* 76: 245–253, 2004.
9. **Dubyak GR.** Purinergic signaling at immunological synapses. *J Auton Nerv Syst* 81: 64–68, 2000.
10. **Dutta AK, Sabirov RZ, Uramoto H, Okada Y.** Role of ATP-conductive anion channel in ATP release from neonatal rat cardiomyocytes in ischaemic or hypoxic conditions. *J Physiol* 559: 799–812, 2004.
11. **Eltzschig HK, Eckle T, Mager A, Küper N, Karcher C, Weissmüller T, Boengler K, Schulz R, Robson SC, Colgan SP.** ATP release from activated neutrophils occurs via connexin 43 and modulates adenosine-dependent endothelial cell function. *Circ Res* 99: 1100–1108, 2006.
12. **Fredholm BB.** Purines and neutrophil leukocytes. *Gen Pharmacol* 28: 345–350, 1997.
13. **Hayashi S, Hazama A, Dutta AK, Sabirov RZ, Okada Y.** Detecting ATP release by a biosensor method. *Sci STKE* 258: 14, 2004.
14. **Hazama A, Hayashi S, Okada Y.** Cell surface measurements of ATP release from single pancreatic beta cells using a novel biosensor technique. *Pflügers Arch* 437: 31–35, 1998.
15. **Ito Y, Son M, Sato S, Ishikawa T, Kondo M, Nakayama S, Shimokata K, Kume H.** ATP release triggered by activation of the $Ca^{2+}$-activated $K^+$ channel in human airway Calu-3 cells. *Am J Respir Cell Mol Biol* 30: 388–395, 2004.
16. **Junger W, Hoyt D, Davis RE, Herdon-Remelius C, Namiki S, Junger H, Loomis W, Altman A.** Hypertonicity regulates the function of human neutrophils by modulating chemoattractant receptor signaling, and activating mitogen-activated protein kinase p38. *J Clin Invest* 101: 2768–2779, 1998.
17. **Lazarowski ER, Boucher RC, Harden TK.** Constitutive release of ATP and evidence for major contribution of ecto-nucleotide pyrophosphatase and nucleoside diphosphokinase to extracellular nucleotide concentrations. *J Biol Chem* 275: 31061–31068, 2000.
18. **Lee SC, Vielhauer NS, Leaver EV, Pappone PA.** Differential regulation of $Ca^{2+}$ signaling and membrane trafficking by multiple P2 receptors in brown adipocytes. *J Membr Biol* 207: 131–142, 2005.
19. **Llaudet E, Hatz S, Droniou M, Dale N.** Microelectrode biosensor for real-time measurement of ATP in biological tissue. *Anal Chem* 77: 3267–3273, 2005.
20. **Loomis WH, Namiki S, Ostrom RS, Insel PA, Junger WG.** Hypertonic stress increases T cell interleukin-2 expression through a mechanism that involves ATP release, P2 receptor, and p38 MAPK activation. *J Biol Chem* 278: 4590–4596, 2003.
21. **Nakamura M, Mie M, Funabashi H, Yamamoto K, Ando J, Kobatake E.** Cell-surface-localized ATP detection with immobilized firefly luciferase. *Anal Biochem* 352: 61–67, 2006.
22. **Neeley WE.** Simple automated determination of serum or plasma glucose by a hexokinase-glucose-6-phosphate dehydrogenase method. *Clin Chem* 18: 509–515, 1972.
23. **North RA, Verkhratsky A.** Purinergic transmission in the central nervous system. *Pflügers Arch* 452: 479–485, 2006.
24. **Olson L, Alund M, Norberg KA.** Fluorescence-microscopical demonstration of a population of gastro-intestinal nerve fibres with a selective affinity for quinacrine. *Cell Tissue Res* 171: 407–423, 1976.
25. **Ostrom RS, Gregorian C, Insel PA.** Cellular release of and response to ATP as key determinants of the set-point of signal transduction pathways. *J Biol Chem* 275: 11735–11739, 2000.
26. **Ostrom RS, Gregorian C, Drenan RM, Gabot K, Rana BK, Insel PA.** Key role for constitutive cyclooxygenase-2 of MDCK cells in basal signaling and response to released ATP. *Am J Physiol Cell Physiol* 281: C524–C531, 2001.
27. **Pellegatti P, Falzoni S, Pinton P, Rizzuto R, Di Virgilio F.** A novel recombinant plasma membrane-targeted luciferase reveals a new pathway for ATP secretion. *Mol Biol Cell* 16: 3659–3665, 2005.
28. **Piston DW, Knobel SM.** Real-time analysis of glucose metabolism by microscopy. *Trends Endocrinol Metab* 10: 413–417, 1999.
29. **Purich DL, Fromm HJ, Rudolph FB.** The hexokinases: kinetic, physical, and regulatory properties. *Adv Enzymol Relat Areas Mol Biol* 39: 249–326, 1973.
30. **Schwiebert EM, Zsembery A.** Extracellular ATP as a signaling molecule for epithelial cells. *Biochim Biophys Acta* 1615: 7–32, 2003.
31. **Sorensen CE, Novak I.** Visualization of ATP release in pancreatic acini in response to cholinergic stimulus. Use of fluorescent probes and confocal microscopy. *J Biol Chem* 276: 32925–32932, 2001.
32. **Stout CE, Costantin JL, Naus CC, Charles AC.** Intercellular calcium signaling in astrocytes via ATP release through connexin hemichannels. *J Biol Chem* 277: 10482–10488, 2002.
33. **Tsai CS, Chen Q.** Purification and kinetic characterization of hexokinase and glucose-6-phosphate dehydrogenase from *Schizosaccharomyces pombe*. *Biochem Cell Biol* 76: 107–113, 1998.
34. **Yegutkin G, Bodin P, Burnstock G.** Effect of shear stress on the release of soluble ecto-enzymes ATPase and 5′-nucleotidase along with endogenous ATP from vascular endothelial cells. *Br J Pharmacol* 129: 921–926, 2000.
35. **Yip L, Cheung CW, Corriden R, Chen Y, Insel PA, Junger WG.** Hypertonic stress regulates T-cell function by the opposing actions of extracellular adenosine triphosphate and adenosine. *Shock* 27: 242–250, 2007.
36. **Zimmermann H.** Extracellular metabolism of ATP and other nucleotides. *Naunyn Schmiedebergs Arch Pharmacol* 362: 299–309, 2000.



Downloaded from http://ajpcell.physiology.org/ by 10.220.33.3 on September 23, 2017